JJMIE

Volume 16, Number 1, January. 2022
ISSN 1995-6665
Pages 63 - 72

Jordan Journal of Mechanical and Industrial Engineering

Application of Direction Vector Model of Multibody System Dynamics in Sports Posture Positioning

Feng Liu*

College of physical Education, Henan University, Kaifeng 475000, China

Received 14 July 2021 *Accepted 22 December 2021*

Abstract

Conventional sports posture positioning method, using convolution neural network, only uses Fast RCNN algorithm to locate sports posture, which leads to low accuracy of sports posture positioning. This paper proposes the application of multi-body system dynamic direction vector model in sports posture positioning. In this paper, the direction vector model of multi-body system dynamics is used to design the constraint of direction vector property and hinge between objects, calculate the activity of objects, and establish the motion posture model; The four coordinate systems of image, pixel, camera and world are established, and the spatial relationship of the four coordinate systems is calculated to complete the spatial transformation of each coordinate system; The gray transformation is carried out for the image to obtain an image. Gray human body image is used to obtain the target image and extract the contour of human body region; Similar to Fast RCNN algorithm and multi-scale context information are used to form a multi scale convolution neural network to locate the sports posture. The experimental results show that positioning sports posture has better positioning effect, higher positioning accuracy and faster positioning efficiency.

© 2022 Jordan Journal of Mechanical and Industrial Engineering. All rights reserved

Keywords: Multi Body System Dynamics; Direction Vector Model; Athletic Sports; Attitude Positioning;

1. Introduction

In the process of training, athletes need to achieve the correct posture standard and the correct position of force. In addition, in the process of sports, the winning and losing of sports also need to be judged according to the posture of the athletes. It is difficult to accurately judge the sports posture of the athletes, especially football and basketball, etc. at the speed of speed the sports events with speed endurance and endurance are the most important. With the development of the times, the competition of these kinds of events is becoming more and more intense, the conversion of attack and defense becomes faster and faster. It is difficult to judge the athletes' movement posture and correct the athletes' movements by the coach naked eye. In the course of the competition, it is difficult for the referee to judge whether the athletes violate the rules of the competition according to the competition process the image, affect the result of sports match judgment. Therefore, some experts put forward the word "posture orientation" to improve the training efficiency, reduce the physical injury of athletes, ensure the fair competition, and have far-reaching significance for improving the teaching and competitive level of sports. Therefore, the orientation of sports posture has become a hot topic in the relevant departments.

With the development of sports posture positioning method, the camera and computer technology are combined. In the training and competition field, more than two cameras are used to locate the whole game image. According to the whole game image, the players' moving position, time and other data are accurately determined, and these data are automatically converted into moving speed and distance, so as to locate the athletes' Sports posture [1, 2]. Sup (Sport universal) is used, the software includes two parts: analysis software and advanced camera [3]. The advanced camera has the function of thermal imaging. It only needs to install the advanced camera in the training and competition field to record the whole process of the competition. Through the analysis software decomposition in sup, we can get the athletes' movement data and estimate the athletes' position, each set of sup at least reaches several million, and needs special personnel to debug and install, which leads to the problem of large-scale promotion of the software. The emitter and upper computer are located safely on the athletes [4]. According to the athletes' sports video captured by the camera, the sports field is gridded, the first rectangular coordinate system is established, and the reference node is designed. The transmitter and upper computer on the athletes are determined, and the

* Corresponding author e-mail: liufeng810107@163.com.

constant values of RF parameters and signal transmission are determined. The distance and seat distance between the athletes' position and each reference node are calculated. However, this method needs to constantly determine the position of the athletes, needs a lot of time to calculate the position of the athletes, and affects the positioning accuracy of the athletes' Sports posture. Taking volleyball players as an example, we collected volleyball players' sports videos, used the background difference theory to obtain the regional position of the players' Sports posture, and divided the volleyball players' sports videos into the color histogram and the gradient direction histogram according to the color and video gradient, and fused the two histograms to determine the regional position of the players and calculate the posture [5]. The weight of the target region feature is used to get the athletes' Sports posture and background feature components, so as to locate the athletes' Sports posture. This method needs less calculation, but it has the problem of low reliability of posture target. Literature uses the average frame difference technology to locate the athletes' Sports posture. It also uses the average frame difference technology to detect the athletes' region in the video based on the athletes' sports video. According to the characteristics of the distribution of the mark points, it uses the horizontal projection theory to separate the mark points and non mark points in the athletes' region. Combined with the distribution law of the mark points, it uses the K-means clustering algorithm. This method is relatively simple, but it has the problem of low positioning accuracy.

In view of the problems in the above research, multi-body system dynamics is introduced to locate the coordinates of athletes in the process of sports, study the rules of athletes' sports, and then combine with the direction vector. By using the compatibility of proper direction and the characteristics of easy programming, the direction vector model of multi-body system dynamics is established to locate the athletes' Sports posture, and the multi-body system dynamics is proposed the application of mechanical direction vector model in sports posture positioning.

2. Sports Posture Positioning Method Based on Direction Vector Model of Multi Body System Dynamics

2.1. Motion attitude model based on direction vector model of multibody system dynamics

Suppose that the dynamics of multi-body system is a multi-body system composed of n_i objects and n_j hinges connected with each other, so the set of objects $B=\{b_1,b_2,\cdots,b_i,\cdots,b_n\}$ is established, where $i=1,2,\cdots,n$, and $j=1,2,\cdots,n$ denote the number of hinges. At this time, select the center of mass b_i in the object set B, take the inertia of the rigid body as the main axis, establish the connected base coordinate system $b_i e_1^{(i)} e_2^{(i)} e_3^{(i)}$, the position vector $r^{(i)}=\left[r_1^{(i)} r_2^{(i)} r_3^{(i)}\right]$ of the origin b_i relative to the inertia base oe1, then the kinetic energy E_i of the object set B is:

$$E_i=\frac{1}{2}\int_E p\dot{r}_p^{(i)T}\dot{r}_p^{(i)}dE=\frac{1}{2}\dot{r}^{(i)T}m_i\dot{r}^{(i)}+\frac{1}{2}\sum_{j=1}^{3}\dot{e}_j^{(i)T}\Pi_j\dot{e}_j^{(i)}=\frac{1}{2}\dot{q}^{(i)T}M_i\dot{q}^{(i)} \tag{1}$$

In Formula (1), E is the potential energy matrix of object set B, and $E=V\left(q^{(i)}\right)$; dE is the integral of potential energy matrix E; $\dot{r}_p^{(i)}=\dot{r}^{(i)}+\sum_{j=1}^{3}\dot{e}_j^{(i)}$ is the absolute velocity of any point p on object set B; $\dot{q}^{(i)}=\left[\dot{r}^{(i)T},\dot{e}^{(i)T}\right]^T$, $e^{(i)}=\left[e_1^{(i)T}e_2^{(i)T}e_3^{(i)T}\right]$, $e_j^{(i)}=\left[e_{1j}^{(i)}e_{2j}^{(i)}e_{3j}^{(i)}\right]$, $j=1,2,3$, $M_i=diag\left(m_iE,\Pi_1^{(i)}E,\Pi_2^{(i)}E,\Pi_3^{(i)}E\right)$, $m_i=\int_E pdE,\Pi_j^{(i)}=\int_E pdE$ [6]. In this case, the constraints on the multi rigid body system composed of n_i objects and n_j joints can be divided into two parts: the constraints on the properties of direction vector and the constraints on the joints between objects, in the formula, the direction vector property constraint ψ is:

$$\psi^{(i)}=\begin{bmatrix}\frac{1}{2}\left(e_1^{(i)T}e_1^{(i)}-1\right)\\ \frac{1}{2}\left(e_2^{(i)T}e_2^{(i)}-1\right)\\ \frac{1}{2}\left(e_3^{(i)T}e_3^{(i)}-1\right)\\ e_1^{(i)T}e_2^{(i)}\\ e_1^{(i)T}e_3^{(i)}\\ e_2^{(i)T}e_3^{(i)}\end{bmatrix} \tag{2}$$

The constraints of joints between objects are more than the constraints of directional vector properties, which can be roughly divided into the following: (1) Suppose that any vector a_i and a_j on the joints between objects are perpendicular, $\psi\left(a_i,a_j\right)=a_i^Ta_j=0$; (2) Assuming that the

relative vector of any two points on the hinge between objects is φ_{ij}, $\psi\left(a_i,\varphi_{ij}\right)=a_i^T\varphi_{ij}=0$ when the vector a_i is perpendicular to φ_{ij}; (3) Suppose that the hinge points between objects are d_i and d_j, when two hinge points d_i and d_j coincide, $\psi\left(d_i,d_j\right)=r_p^{(j)}-r_p^{(i)}=0$; When the distance between two hinge points d_i and d_j remains unchanged, $\psi\left(d_i,d_j\right)=\varphi_{ij}^T\varphi_{ij}-b^2=0$; (4) It is assumed that there is a consolidated coordinate system $\left(d_if_ig_ih_i,d_jf_jg_jh_j\right)$ between the two hinge points d_i and d_j, where $f_ig_ih_i$ and $f_jg_jh_j$ both represent parallel vectors, $\psi\left(h_i,h_j\right)=\begin{bmatrix}\psi\left[f_i,h_j\right]\\ \psi\left[g_i,h_j\right]\end{bmatrix}=0$ when h_i and h_j are parallel to each other; $\psi\left(h_i,\varphi_{ij}\right)=\begin{bmatrix}\psi\left[f_i,\varphi_{ij}\right]\\ \psi\left[g_i,\varphi_{ij}\right]\end{bmatrix}=0$ when h_i and φ_{ij} are parallel.

By substituting the above constraints into Formula (1), Formula (1) can be regarded as the direction vector model of multibody system dynamics. At this time, the object and the hinge between the objects in the above calculation process represent the athlete's limbs and trunk respectively. At this time, the direction vector model of multi-body system dynamics shown in Formula (1) is the athlete's motion posture model.

2.2. Determine camera coordinate system

Before camera calibration, the camera model must be established. According to the simplest pinhole imaging principle, the light in the scene passes through the camera aperture, and then hits the CCD sensor on the back of the camera to get the corresponding image [7]. Therefore, four coordinate systems are established as follows: (1) Image coordinate system $\left(x,y\right)$; (2) Pixel coordinate system $\left(o,v\right)$; (3) Camera coordinate system $\left(X_1,Y_1,Z_1\right)$; (4) World coordinate system $\left(X_2,Y_2,Z_2\right)$. Calculate the spatial relationship of the four coordinate systems, and complete the spatial transformation of each coordinate system.

The spatial relationship between image coordinate system $\left(x,y\right)$ and pixel coordinate system $\left(o,v\right)$. The position relationship between image coordinate system and pixel coordinate system can be divided into vertical and non-vertical. When the two coordinate axes are perpendicular to each other, there is a relationship between coordinate systems as shown in the following formula:

$$\begin{cases}o=\dfrac{x}{d_x}+o_0\\ v=\dfrac{y}{d_y}+v_0\end{cases}\tag{3}$$

In Formula (3), d_x represents the actual size of the pixel in the x-axis direction; d_y represents the actual size of the pixel in the y-axis direction; $\left(o_0,v_0\right)$ represents a coordinate position in the pixel coordinate system $\left(o,v\right)$ [8]. In general, the two axes of the position relationship between the image coordinate system and the pixel coordinate system are not perpendicular to each other, and there is a certain angle θ, then:

$$\begin{aligned}o&=o_0+\frac{x_d}{d_x}-\frac{y_d cot\theta}{d_x}\\ v&=v_0+\frac{y_d}{d_y sin\theta}\end{aligned}\tag{4}$$

The spatial relationship between camera coordinate system $\left(X_1,Y_1,Z_1\right)$ and image coordinate system $\left(x,y\right)$. The X_1 and Y_1 axes of the camera coordinate system should be parallel to the x and y axes of the image coordinate system, while the Z_1 axis of the camera coordinate system is the optical axis. According to the similarity principle of triangles, it can be concluded that:

$$Z_1 \cdot \begin{bmatrix} x \\ y \\ 1 \end{bmatrix} = \begin{bmatrix} f & 0 & 0 & 0 \\ 0 & f & 0 & 0 \\ 0 & 0 & 1 & 0 \end{bmatrix} \cdot \begin{bmatrix} X_1 \\ Y_1 \\ Z_1 \\ 1 \end{bmatrix} \quad (5)$$

The spatial relationship between camera coordinate system (X_1, Y_1, Z_1) and world coordinate system (X_2, Y_2, Z_2). The world coordinate system will associate the image coordinate system, pixel coordinate system, camera coordinate system with the space object. According to the transformation principle of the space coordinate system, the following relationship can be obtained:

$$\begin{bmatrix} X_1 \\ Y_1 \\ Z_1 \end{bmatrix} = \begin{bmatrix} T & \varepsilon \\ 0 & 1 \end{bmatrix} \cdot \begin{bmatrix} X_2 \\ Y_2 \\ Z_2 \\ 1 \end{bmatrix} \quad (6)$$

In Formula (6), T represents the rotation matrix, which belongs to the orthogonal unit matrix with the size of 3 * 3; ε represents the three-dimensional vector [9]. By synthesizing the above four calculation formulas, the relationship between the four coordinate systems is obtained, so as to obtain the coordinate system of the equipment in the process of athletes' sports, determine the coordinates of the camera position of the athletes, obtain the target image, and extract the contour of the human body region.

2.3. Extracting the contour of human body region from the target image

According to the collected sports video sequence, we need to select the image of the motion posture to be located as the target image of the motion posture positioning. Therefore, on the basis of the determined position of the camera to capture the athletes' Sports posture image, the gray-scale transformation of the image is carried out, and a gray-scale human body image is obtained. Then m consecutive image sequences $f_t(t = 1, 2, \cdots, m)$ are selected from the video data. Suppose that the gray value of a pixel (x, y) on the j-th image is $G_j(x, y)$, then for the m-th image sequence, the average gray value of the pixel (x, y) is:

$$\bar{G}_j(x, y) = \frac{1}{m} \sum_{j=1}^{m} G_j(x, y) \quad (7)$$

Using Formula (7), the average gray values $\bar{G}_1(x, y)$, $\bar{G}_2(x, y)$, ⋯, $\bar{G}_m(x, y)$ of m image sequences on each pixel point are calculated in turn. Then the new image composed of pixels with average gray values is the calculated background image.

After obtaining the target image and the background image, we can use the background difference method to calculate the difference between the target image and the background image, so as to obtain the contour of the human body. Set a frame containing the human body selected from the video data to $H(x, y)$ after gray conversion, and the obtained background image is $G(x, y)$, and the threshold value is D, then:

$$\begin{cases} (x, y) \in \textit{target if } |H(x, y) - G(x, y)| > D \\ (x, y) \in \textit{background} \qquad \textit{others} \end{cases} \quad (8)$$

Usually, there are isolated noise points of different sizes in the human body region obtained by background difference method, which will interfere with the subsequent processing and affect the effect of human contour extraction. The commonly used solution is to use median filter to denoise the preliminary human body region image [10]. Median filtering uses the median value of the gray value of all pixels in the neighborhood window of a pixel to replace the gray value of the pixel, which has a good effect on eliminating the noise points in the extracted human body region image [11].

Some human body region images will appear cavity, fracture or loss of some parts of the human body during processing [12]. Therefore, it needs to be repaired. The usual method is to use the image morphology methods such as dilation operation and erosion operation to deal with the unsatisfactory human body region image. Firstly, the denoised human body image is expanded to fill the small holes, then:

$$X \oplus Y = \{u \in \gamma^2, u = x + g, x \in X\} \quad (9)$$

In Formula (9), γ^2 represents the two-dimensional space of the human body region image; u represents a point in the human body region image; x represents any point in the pixel (x, y), X represents the set of pixel (x, y), and g represents the hole position in the background image [13]. Next, the image of human body region is corroded to eliminate the noise of small area, then:

$$X \ominus Y = \{u \in \gamma^2, u + g \in X\} \quad (10)$$

After the human body region image is restored by morphological method, it is binarized:

$$g(x,y)=\begin{cases}0 & spot(x,y)\in Contour\ area\\ 1 & spot(x,y)\notin Contour\ area\end{cases} \quad (11)$$

By synthesizing the Formula (5), the contour extraction of the positioning target is completed, and the clarity of the extracted contour can be guaranteed. At this time, only according to the movement posture model, we can locate the posture of athletes in sports.

2.4. Positioning the posture of sports

In this study, the multi-scale convolution neural network will be used to locate the sports posture based on the movement posture model. The multi-scale convolutional neural network is composed of a candidate frame generation sub network and a positioning sub network [14]. The candidate frame can be generated at different levels in the sub network by using a small positioning network to generate candidate frames of different scales [15]. Therefore, in the positioning sub network, the candidate box output from the sub network is used as the input. In the multi-scale convolution neural network algorithm, the candidate frame is generated into a sub network. In four convolution layers with different depths, the candidate frame is generated for the target. Each small network only trains the training samples within a certain scale, ignoring the contribution of the target outside the scale to the small network. Assume that the whole training set is $S=\{S_1,S_2,\cdots,S_k\}$, and S_k is the sample set contained in scale k, which only contributes to the k-th small location network. The loss function of the network is defined as follows:

$$L(\eta)=\sum_{k=1}^{4}\sum_{i\in S_k} w_k\left(l\left(I(X),U\right)+\delta[U=1]l(q,\tilde{q})\right) \quad (12)$$

In Formula (12), $L(\eta)$ is the loss of multi-scale convolutional neural network; η is the learning parameter of the network; w_k is the weight of k range of each scale; l_1 is the classification loss; $I(X)$ is a function of predicting classification probability and the real label U; l_2 is the regression loss of rectangular box, which is a function of positive sample prediction box $\tilde{q}$ and real box q; δ is the weight parameter representing the regression loss of positive sample rectangle [16].

According to the multi-scale convolutional neural network structure selected above, the network loss function calculation formula is determined, and the Fast RCNN algorithm is used to locate the final sports posture. The convolution layer backbone is shared with the convolution layer of the candidate frame generation sub network, which only extracts the features used to locate the motion posture in the conv4-3 layer of the convolution backbone, and the definition of the loss function is the same as that of the Fast RCNN algorithm, which is divided into classification loss and rectangular frame regression loss [17]. Different from Fast RCNN algorithm, deconvolution operation and single scale context information extraction strategy are used in sports posture positioning sub network.

Due to the great difference of sports posture, the scale span of sports posture to be located is large. In the process of sports, many athletes are far away from the sports field monitoring, resulting in their scale in the image area is very small. Suppose a pedestrian target with a width of 32 pixels, its characteristic width in the fourth convolution layer is only eight times of the original 1. Only 4 pixels are occupied in the feature map [18]. At this time, ROI-pooling will introduce large feature error. Therefore, the feature graph is up sampled to avoid the introduction of additional parameters and computational complexity.

Based on the above analysis, according to the extracted sports posture positioning target and the analysis results of sports posture model, in the selected multi-scale convolution neural network, multi-scale extraction context information is used to help multi-scale convolution neural network locate sports posture [19]. Because the “multi-scale” in the multi-scale convolution neural network algorithm is mainly reflected in the candidate frame generation sub network, but in the target positioning sub network, it only extracts features in one convolution network layer, which ignores a very important concept of deep convolution network, that is, the features of different convolution layers express different levels of information in the image.

The convolution layer of deep convolution neural network uses the learned template to carry out linear transformation on the pixels in the input image in the form of sliding window. From the perspective of network structure, multiple convolution layers are connected in a cascade way, that is, the template is used to continuously carry out linear transformation on the transformed image [20]. After visualizing these different levels of features, we can get the conclusion that the shallow convolution layer output generally contains more local edge information, which is not robust to noise, while the deep convolution layer output contains semantic information about the whole image [21, 22]. Although many details are ignored, the semantic judgment of the target is relatively robust. These features of different levels are simply connected together. For the convoluted feature map of different levels, the corresponding feature map area of the sample is found in the feature map, and then the feature of the area is extracted by ROI-pooling method, and these features are stacked together by

 © 2022 Jordan Journal of Mechanical and Industrial Engineering. All rights reserved

the connection layer, so that the target is easy to understand A convolution layer is used to simplify the parameters of these features, and finally the full connection layer is used for classification and rectangular box regression. So far, the positioning of sports posture is completed.

Definitions of all the variables in the text are shown in Table 1.

Table 1. Variable definition

Symbol abbreviation	Meaning
n_i	objects
n_j	hinges
B	the set of objects
i, j	the number of hinges
b_i	the center of mass in the object set B
$b_i e_1^{(i)} e_2^{(i)} e_3^{(i)}$	the base coordinate system
$r^{(i)}$	the position vector relative to the inertial base
E	the potential energy matrix of the target set
dE	the integrals of the potential energy matrix
p	any point in the collection B
$\dot{r}_p^{(i)}$	the absolute speed of any point p
ψ	the property constraint for the direction vector
a_i , a_j	any arbitrary vector of the nodes between objects
φ_{ij}	relative vector of any two points on the hinge between objects
d_i , d_j	the hinge points between objects
$f_i g_i h_i$, $f_j g_j h_j$	the parallel vectors between the two hinge points d_i and d_j
(x, y)	the image coordinate system
(o, v)	the pixel coordinate system
(X_1, Y_1, Z_1)	the camera coordinate system
(X_2, Y_2, Z_2)	the world coordinate system
d_x	the actual size of the pixel in the x -axis direction
d_y	the actual size of the pixel in the y -axis direction
(o_0, v_0)	the coordinate position in the pixel coordinate system (o, v)
θ	the horizontal and vertical axis angle between image system and pixel system
T	the orthogonal rotation matrix of size 3 * 3
ε	three-dimensional vector
f_t	the serial sequence of continuous images selected from the video data
m	the number of image sequences
$G_j(x, y)$	the gray value of a pixel (x, y) on the j -th image
$\bar{G}_j(x, y)$	the average gray value of the pixel (x, y)
$H(x, y)$	all frame sets after image gray scale conversion selected from the video data
$G(x, y)$	the grayscale-transformed background images
D	the threshold value for the grayscale conversion
γ^2	the two-dimensional space of the human body region image
u	a point in the human body region image
X	the set of pixel (x, y)
g	the hole position in the background
k	ratio scale
S_k	the sample sets trained by proportion in convolutional neural networks
$L(\eta)$	the loss of multi-scale convolutional neural network
η	the learning parameter of the network
w_k	the weight of k range of each scale
l_1	the classification loss
U	the real label
$I(X)$	a function of predicting classification probability and the real label U
$\tilde{q}$	the positive sample prediction box
q	the real box
l_2	the regression loss of rectangular box, which is a function of positive sample prediction box $\tilde{q}$ and real box q
δ	the weight parameter representing the regression loss of positive sample rectangle

3. Experimental Results and Analysis

Three groups of conventional sports posture positioning methods were selected, and EOS C300 Mark 2 high-definition camera was used to collect the far mobilization video of volleyball. Taking the movement posture of volleyball players in sports as the experimental object, the sports posture positioning method based on multi-body system dynamics direction vector model was verified. Compare four groups of sports posture positioning methods, positioning sports posture performance.

3.1. Experimental preparation

According to this experiment, the experimental camera EOS C300 Mark 2 HD camera is shown in Figure 1.

Figure 1. EOS C300 Mark 2 HD camera

The parameters of EOS C300 Mark 2 HD camera are shown in Table 2.

Table 2. Parameters of EOS C300 Mark 2 HD camera

Product configuration		Specifications
Sensor	Type	Super 35mmcmos single chip sensor
	Total prime number	nine million eight hundred and forty thousand
	Effective pixel	eight million eight hundred and fifty thousand
Camera lens	Filter	RGB primary filter
	Bayonet type	EF bayonet
	Support lens	EF LENS, EF cinema lens
Exposure control	Exposure mode	Manual/single automatic aperture/automatic aperture control
	Shutter settings	Speed, angle, clear scan, slow or off
	Aperture setting	Manual setting (you can choose to set in 1/2 or 1/3 or fine display setting)
	ISO sensitivity setting	Iso100*-102400* (extended sensitivity)
	Gain setting	Normal setting (-6 db to 54 db*) Fine setting (can be set in 0.5 dB between -6 db and 54 db)
	ND filter	Built in, electric, 5 density settings (2, 4, 6, 8*, 10*)
Video storage format		CFAST card record video format

Under the condition of EOS C300 Mark 2 high-definition camera parameters as shown in Table 2, the collected volleyball player sports video sequence contains a total of 500 images. From these 500 images, 200 images are selected as training samples and 300 images are selected as test samples. The selected volleyball player sports video sequence image example is shown in Figure 2.

According to the experimental object shown in Figure 2, the four groups of sports posture positioning methods need to be run on the computer to locate the volleyball players' Sports posture. Therefore, the operation environment of the four groups of positioning methods is designed as shown in Table 3.

Figure 2. Example of video sequence image of Volleyball Players

Table 3. Operation environment of four groups of positioning methods

Environment	To configure	Specifications
Hardware environment	Hard disk	500 GB/5400 rpm
	Memory	DDR3 4G
	Processor	Intel Core i5 2.4 GHz processor
	Graphics card	Intel(R) HD Graphics 3000
Software environment	Operating environment	Windows 7, 64 bit operating system
	Development environment	MATLAB language, MATLAB R2012b software

Based on the experimental object selected in this experiment and the designed experimental environment, four groups of sports posture positioning methods are used to locate the volleyball players' Sports posture respectively. The four groups of sports posture positioning methods are compared to locate the volleyball players' Sports posture effect, efficiency and accuracy. The experimental results and experimental process are as follows.

3.2. Experimental result

3.2.1. The first group of experimental results

Four groups of positioning methods are used to locate the volleyball players' movement posture in the video sequence image example of volleyball players as shown in Figure 2, and the positioning results of volleyball players' movement posture are calibrated, so as to judge the four groups of sports posture positioning methods and locate the effect of volleyball players' movement posture. The experimental results are shown in Figure 3.

It can be seen from Figure 3 that the three groups of conventional methods can only locate the movement posture of volleyball players by a large margin, but the positioning range of conventional method 1 is wide, which objectively shows that the positioning accuracy of conventional method 1 is low, and the positioning range of conventional method 2 is wide. Conventional method 1 is small,

which objectively indicates that conventional method 2 has high accuracy in positioning volleyball players' motion posture; Conventional method 3 has deviation in positioning volleyball players' motion posture, when the distance between two players is relatively close, the two players' motion posture will be positioned together, which objectively indicates that conventional method 3 is extremely low in positioning volleyball players' motion posture; However, the research method is limited Positioning the movement posture of volleyball players, as long as the players have movement posture, they will be positioned to the movement posture of volleyball players, and the positioning range is small, so the movement posture of each part of the players can be positioned separately. It can be seen that the research of sports posture positioning method, positioning the athletes of all parts of the movement posture effect is better.

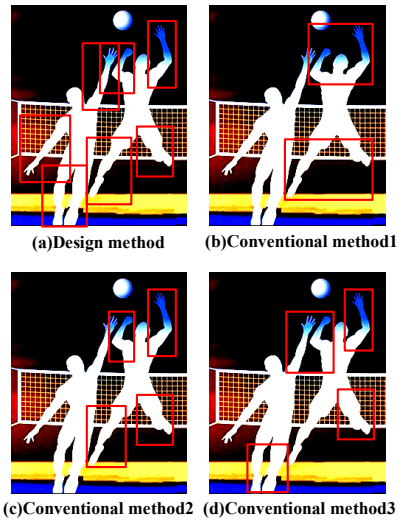

Figure 3. The effect of four groups of methods in positioning volleyball players' movement posture

3.2.2. The second group of experimental results

On the basis of the first group of experiments, the second group of experiments was carried out to calculate the accuracy of the four groups of positioning methods in positioning the movement posture of volleyball players, and to verify the accuracy of the four groups of positioning methods in positioning the movement posture of volleyball players. In this experiment, a total of 300 video sequence images of volleyball players as shown in Figure 2 are selected as the sample data of this group of experiments to test the accuracy of four groups of positioning methods to locate different numbers of volleyball players' movement posture samples. In order to ensure the preciseness of the experiment, the positioning accuracy is recorded every 25 volleyball players' movement posture images, including the first and last experimental values. The experimental results are shown in Table 4.

Table 4. The correct rate of positioning volleyball players' movement posture with four groups of positioning methods

Number of experimental samples	Design method (%)	Conventional method 1 (%)	Conventional method 2 (%)	Conventional method 3 (%)
1 sheet	97.8	94.6	93.6	92.5
25 sheet	97.6	95.1	93.0	92.6
50 sheet	97.0	94.3	93.3	93.0
75 sheet	97.9	94.5	93.5	94.7
100 sheet	97.4	95.0	93.7	92.9
125 sheet	97.5	93.9	93.0	94.0
150 sheet	98.0	94.2	92.9	92.8
175 sheet	97.6	94.9	93.2	94.1
200 sheet	97.7	93.8	93.3	92.7
225 sheet	97.5	94.1	93.5	92.5
250 sheet	98.0	94.5	94.0	93.3
275 sheet	97.3	94.3	94.1	92.8
300 sheet	97.7	94.2	93.2	92.7

It can be seen from Table 4 that the difference between the maximum and minimum values of the conventional method 1 is 1.3%, with an average of 94.4%; The difference between the maximum and minimum values of the conventional method 2 is 1.2%, with an average of 93.4%; The difference between the conventional method 3 and the conventional method 3 is 1.2%. The results show that the difference between the maximum and minimum value of the correct rate of the sample is 2.2%, with an average of 93.1%; The difference between the maximum and minimum value of the correct rate of the sample is 1%, with an average of 97.6%; It can be seen that the correct rate of the sample of the different number of volleyball players is the highest. The differences between the maximum and minimum values were 0.3%, 0.2% and 1.2% smaller than those of the three conventional methods, and the average values were 3.2%, 4.2% and 4.5% smaller than those of the three conventional methods. Therefore, the accuracy of the research method is significantly higher than that of the three conventional methods.

3.2.3. The third group of experimental results

On the basis of the first group and the second group of experiments, the third group of experiments is carried out to calculate the positioning time of the four groups of positioning methods to locate the volleyball players' movement posture and verify the efficiency of the four groups of positioning methods to locate the volleyball players' movement posture. In this experiment, 300 video sequence images of volleyball players as shown in Figure 2 are also selected as the sample data of this group of experiments to test the time for four groups of positioning methods to locate different numbers of samples of volleyball players' movement posture. In order to ensure the preciseness of the experiment, the positioning accuracy is recorded every 25 volleyball players' movement posture images, including the

first and last experimental values. The experimental results are shown in Table 5.

Table 5. Positioning time of volleyball players' movement posture by four groups of positioning methods

Number of experimental samples	Design method (s)	conventional method 1 (s)	conventional method 2 (s)	conventional method 3 (s)
1 sheet	0.62	1.57	1.10	1.05
25 sheet	1.31	2.56	1.75	1.81
50 sheet	1.62	3.40	2.51	2.58
75 sheet	2.35	4.34	2.99	3.28
100 sheet	2.65	5.06	3.35	3.98
125 sheet	3.23	5.99	3.81	4.11
150 sheet	3.75	7.53	4.58	4.92
175 sheet	4.30	8.14	5.35	5.57
200 sheet	4.98	8.96	5.98	6.02
225 sheet	5.57	9.70	6.72	6.97
250 sheet	6.34	10.03	7.12	7.85
275 sheet	6.91	10.94	7.95	8.95
300 sheet	7.89	11.42	8.70	9.87

It can be seen from Table 5 that with the increase of the number of volleyball players' movement posture samples, the positioning experiment increases. Among them, the difference between the maximum and minimum values of routine method 1 is 9.85 s, and the average value is 6.9 s; The difference between the maximum and minimum of the sample time of different number of volleyball players' movement posture is 7.6 s, with an average of 4.8 s; The difference between the maximum and minimum of the sample time of different number of volleyball players' movement posture is 8.82 s, with an average of 5.2 s; The difference between the sample time of different number of volleyball players' movement posture is 8.82 s, with an average of 5.2 s. The difference between the minimum value and the maximum value is 7.27 s, and the average value is 4.0 s. It can be seen that the difference between the maximum and minimum values of different number of volleyball players' movement posture sample time is 2.58 s, 0.33 s, 1.55 s less than the three groups of conventional methods, and the average value is 2.9 s, 0.8 s, 1.2 s less than the three groups of conventional methods. Therefore, the efficiency of the research method is significantly higher than that of the three conventional methods.

Based on the above three groups of experimental results, we can see that the sports posture positioning method has better positioning effect, higher positioning accuracy and faster positioning efficiency.

4. Conclusion

This paper applied a directional vector model for the dynamics of many-body systems. The combination of multi-body system dynamics model and direction vector, constitute a multi-body system dynamics direction vector model, determine the athletes in the process of sports, limbs, trunk and head and other parts, the existence of the movement law and direction. The experimental results show that this method improved the positioning effect of the motor posture, provided with a better positioning accuracy, shortened the positioning time, and provided with a theoretical reference for the coach to accurately judge the movement posture and correct the athlete movements. However, there are still some deficiencies in this research. In the future research, we need to further study the constraint information of joint points in the sports posture positioning method, solve some depth differences, and further improve the positioning accuracy.

References

[1] Zhu Y, Zhang T, Xu S, et al. A calibration method of USBL installation error based on attitude determination. IEEE Transactions on Vehicular Technology, 2020, 69(8): 8317-8328.

[2] Wang D, Liu A, Xia X. New method for airborne SAR image positioning. The Journal of Engineering, 2019, 2019(19): 6021-6023.

[3] Shi B, Zhang F, Yang F, et al. A positioning error compensation method for a mobile measurement system based on plane control. Sensors, 2020, 20(1): 294.

[4] Xu X, Liu X, Zhao B, et al. An extensible positioning system for locating mobile robots in unfamiliar environments. Sensors, 2019, 19(18): 4025.

[5] Zheng Y, Li Q, Wang C, et al. Magnetic-Based positioning system for moving target with feature vector. IEEE Access, 2020, 8: 105472-105483.

[6] Lee M, Szuttor K, Holm C. A computational model for bacterial run-and-tumble motion. The Journal of Chemical Physics, 2019, 150(17): 174111.

[7] Xu H, Yan R. Research on sports action recognition system based on cluster regression and improved ISA deep network. Journal of Intelligent and Fuzzy Systems, 2020, 39(4): 5871-5881.

[8] Amin S M. A new robust combined control system for improving manoeuvrability, lateral stability and rollover prevention of a vehicle. Proceedings of the Institution of Mechanical Engineers, Part K: Journal of Multi-body Dynamics, 2019, 234(1): 198-213.

[9] Sannikova T N, Kholshevnikov K V. The averaged equations of motion in the presence of an inverse-square perturbing acceleration. Astronomy Reports, 2019, 63(5): 420-432.

[10] Al-Solihat M K, Behdinan K. Nonlinear dynamic response and transmissibility of a flexible rotor system mounted on viscoelastic elements. Nonlinear Dynamics, 2019, 97(2): 1581-1600.

[11] Chebly A, Talj R, Charara A. Coupled longitudinal/lateral controllers for autonomous vehicles navigation, with experimental validation. Control Engineering Practice, 2019, 88: 79-96.

[12] Neves R, Sanchez J P. Multifidelity design of low-thrust resonant captures for near-earth asteroids. Journal of Guidance, Control, and Dynamics, 2019, 42(2): 335-346.

[13] Shvetsov I V, Zhelnov D V, Zubarev Y M. On dynamics and control when finishing body parts. IOP Conference Series Materials Science and Engineering, 2019, 65(12): 012048.

[14] Palikhe S, Kim S, Kim J J. Critical success factors and dynamic modeling of construction labour productivity. International Journal of Civil Engineering Transaction a Civil Engineering, 2019, 17(3): 427-442.
[15] Ramesh R S, Fredette L, Singh R. Identification of multi-dimensional elastic and dissipative properties of elastomeric vibration isolators. Mechanical Systems and Signal Processing, 2019, 118: 696-715.
[16] Takao Y, Mori O, Kawaguchi J. Analysis and design of a spacecraft docking system using a deployable boom. Acta Astronautica, 2021, 179: 172-185.
[17] Lin R, Molignini P, Papariello L, et al. MCTDH-X: The multiconfigurational time-dependent Hartree method for indistinguishable particles software. Quantum Science and Technology, 2020, 5(2): 024004 (16pp).
[18] Ghabraei S, Moradi H, Vossoughi G. Investigation of the effect of the added mass fluctuation and lateral vibration absorbers on the vertical nonlinear vibrations of the offshore wind turbine. Nonlinear Dynamics, 2021, 103: 1499-1515.
[19] Yazdankhoo B, Nikpour M, Beigzadeh B, et al. Improvement of operator position prediction in teleoperation systems with time delay: Simulation and experimental studies on Phantom Omni devices. Jordan Journal of Mechanical and Industrial Engineering, 2019, 13(3): 197-205.
[20] Sòria-Perpinyà X, Urrego P, Pereira-Sandoval M, et al. Monitoring the ecological state of a hypertrophic lake (Albufera of València, Spain) using multitemporal Sentinel-2 images. Limnetica, 2019, 38(1): 457-469.
[21] Rogge T, Jones D, Drossel B, et al. Interplay of spatial dynamics and local adaptation shapes species lifetime distributions and species-area relationships. Theoretical Ecology, 2019, 12(4): 437-451.
[22] Verjans M, Schleer P, Griesbach J, et al. Modelling patient dynamics and controller impact analysis for a novel self-stabilizing patient transport aid. IFAC-PapersOnLine, 2019, 51(34): 208-213.